AIP | Journal of Applied Physics

Two symmetric n-type interfaces SrTiO3/LaAlO3 in perovskite: Electronic properties from density functional theory

A. H. Reshak, M. S. Abu-Jafar, and Y. Al-Douri

Citation: Journal of Applied Physics **119**, 245303 (2016); doi: 10.1063/1.4954293
View online: http://dx.doi.org/10.1063/1.4954293
View Table of Contents: http://scitation.aip.org/content/aip/journal/jap/119/24?ver=pdfcov
Published by the AIP Publishing

Two symmetric n-type interfaces $SrTiO_3/LaAlO_3$ in perovskite: Electronic properties from density functional theory

A. H. Reshak,[1,2,a)] M. S. Abu-Jafar,[3,a)] and Y. Al-Douri[4,5]
[1]*New Technologies—Research Centre, University of West Bohemia, Univerzitni 8, 306 14 Pilsen, Czech Republic*
[2]*Center of Excellence Geopolymer and Green Technology, School of Material Engineering, University Malaysia Perlis, 01007 Kangar, Perlis, Malaysia*
[3]*Department of Physics, An-Najah N. University, P. O. Box 7, Nablus, Palestine*
[4]*Institute of Nano Electronic Engineering, University Malaysia Perlis, 01000 Kangar, Perlis, Malaysia*
[5]*Physics Department, Faculty of Science, University of Sidi-Bel-Abbes, 22000 Sidi-Bel-Abbes, Algeria*

(Received 31 March 2016; accepted 8 June 2016; published online 24 June 2016)

The first principles study of the (001) two symmetric n-type interfaces between two insulating perovskites, the nonpolar $SrTiO_3$ (STO), and the polar $LaAlO_3$ (LAO) was performed. We have analyzed the formation of metallic interface states between the STO and LAO heterointerfaces by using the all-electron full-potential linearized augmented plane-wave approach based on the density functional theory, within the local density approximation, the Perdew-Burke-Ernzerhof generalized gradient approximation (PBE-GGA), and the Engel-Vosko GGA (EVGGA) formalism. It has been found that some bands cross the Fermi energy level (E_F), forming a metallic nature of two symmetric n-type 6.5STO/1.5LAO interfaces with density of states at E_F, $N(E_F)$ of about 3.56 (state/eV/unit cell), and bare electronic specific heat coefficient (γ) of about 0.62 mJ/(mol cell K^2). The electronic band stature and the partial density of states in the vicinity of E_F are mainly originated from Ti1,2,3,4-3dxy orbitals. These bands are responsible for the metallic behavior and the forming of the Fermi surface of the two symmetric n-type 6.5STO/1.5LAO interfaces. To obtain a clear map of the valence band electronic charge density distribution of the two symmetric n-type 6.5STO/1.5LAO interfaces, we have investigated the bond's nature and the interactions between the atoms. It reveals that the charge is attracted towards O atoms as it is clear that the O atoms are surrounded by uniform blue spheres which indicate the maximum charge accumulation. *Published by AIP Publishing*. [http://dx.doi.org/10.1063/1.4954293]

I. INTRODUCTION

Recently, it has been found that the $LaAlO_3$ (LAO) and $SrTiO_3$ (STO) interfaces show numerous promising applications. For instance, it can be applied to quasi-two-dimensional (2D) electron transport with high electron mobility,[1] novel devices and technology, 2D superconductivity at low temperatures,[2] and electric field-tuned metal insulator and superconductor insulator phase transitions.[3] One of the notable examples is the interface between the two band insulators with the perovskite ABO_3 structure, $LaAlO_3$ (LAO), and $SrTiO_3$ (STO).[4] The n-type interface, in which the LAO layer is grown on top of the TiO_2-terminated STO, has highly mobile carriers, while the p-type interface, in which the LAO layer is grown on top of the SrO-terminated STO, is totally insulating.[1] The emergence of conductivity at the $SrTiO_3/LaAlO_3$ interface could be attributed to the intrinsic electronic reconstruction due to the polar discontinuity at the interface.[5] This can be understood in perovskite oxides that have a generic ABO_3 structure, where A and B are metal cations. For STO, A is Sr^{2+} and B is Ti^{4+}, where AO and BO_2 planes are charge-neutral which makes the STO a nonpolar material. Whereas for LAO, A is La^{3+} while B is Al^{3+}, therefore AO and BO_2 planes have +1 and −1 charges, respectively, making the material polar.[6] At the interface of the polar and non-polar materials, the electronic reconstruction could explain the mechanism of electronic conduction.[7] The other probability of emerging the conductivity at the interface is based on the observed intermixing of cations across the $SrTiO_3/LaAlO_3$ interface.[8] The orientation of the channels and their thermal behavior suggests that the $LaAlO_3/SrTiO_3$ (LAO/STO) interface originates as a consequence of the STO tetragonal domain formation which sets in below 105 K.[9,10] The study of the domain structure confirms that the channel-like conductivity in LAO/STO is due to the STO tetragonal domain structure and emphasizes the importance of STO to the interfacial properties. The LAO/STO interface has been extensively investigated experimentally[5,8,10–18] and theoretically[19–21] due to the existence of two kinds of interfaces, $LaO/TiO_2/SrO$ and $SrO/AlO_2/LaO$, therefore attracting a lot of interest in such a system.[22–24] To the best of our knowledge, most investigations on the electronic properties of the $SrTiO_3/LaAlO_3$ interface have been done experimentally and theoretically.[5,10–27] Some literature reports the electronic properties of two symmetric n-type 6.5STO/1.5LAO interfaces,[28–32] but unfortunately none of them report the electronic charge density distribution and the electronic charge transfer. Therefore, a step forward is necessary to understand the origin of the electronic charge density distribution and the electronic

[a)]Authors to whom correspondence should be addressed. Electronic addresses: maalidph@yahoo.co.uk and mabujafar@najah.edu

charge transfer at the interface. We have performed comprehensive theoretical investigations based on the all-electron full potential method within three kinds of exchange correlations: local density approximation (LDA),[33] the Perdew-Burke-Ernzerhof generalized gradient approximation (PBE-GGA),[34] and the Engel-Vosko GGA (EVGGA) formalism.[35] To ascertain the influence of the XC on the resulting properties, EVGGA formalism is the most capable at reproducing the exchange potential at the expense of less agreement in the exchange energy, which yields a better band splitting.

II. DETAILS OF CALCULATIONS

The electronic band structures, density of states, electronic charge density distribution, and the Fermi surface of 6.5STO/1.5LAO superlattices were performed using all-electron full potential linear augmented plane wave (FP-LAPW+lo) method in a scalar relativistic version as embodied in the WIEN2 k code.[36] To solve the exchange-correlation potential, the generalized gradient approximation LDA, PBE-GGA, and EVGGA were used. In FP-LAPW+lo, the unit cell is divided into two regions: the spherical harmonic expansion is used inside the non-overlapping spheres of muffin-tin radius (R_{MT}), while the plane wave basis set was chosen in the interstitial region (IR) of the unit cell. The R_{MT} was chosen to be 2.5, 2.46, 1.83, 1.74, and 1.62 a.u. for La, Sr, Ti, Al, and O, respectively. The $R_{MT} \times K_{max}$ parameter was taken to be 7.0 to determine the matrix size, R_{MT} being the smallest radius of the muffin-tin sphere while K_{max} is the maximum modulus for the reciprocal lattice vectors K. The valence wave functions inside the muffin-tin spheres were expanded up to $l_{max} = 10$, while the charge density was Fourier expanded up to $G_{max} = 12$ (a.u)$^{-1}$. Self-consistency was obtained using 500 $\vec{k}$ points in the irreducible Brillouin zone (IBZ). The self-consistent calculations were converged since the total energy of the system is stable within 0.00001 Ry. The calculations of the electronic band structures were performed within 3000 $\vec{k}$ points in the IBZ. Brillouin zone of the 40 atom supercell was sampled with a $8 \times 8 \times 1$ k-point grid. In our calculations, the two symmetric n-type interface is along the (001) direction so that the z-axis is perpendicular to the interface. GGA method was used to relax the atomic positions in the supercell. We fixed the in-plane lattice constant (parallel to the interface) at the experimental value of STO a = 3.91 Å, while the length of the supercell in the direction normal to the interface (out-of-plane) was taken to be 8 a. Atomic positions have been relaxed for the supercell by minimizing the forces on the atoms. All atoms are allowed to relax in the z direction until the force on each one is smaller than 1 m Ry/a.u. The spin-orbit coupling is not included in our calculations.

III. RESULTS AND DISCUSSION

We have presented the results of the electronic band structure calculations regarding the 6.5STO/1.5LAO superlattices. We built a symmetric supercell, with one AlO_2 layer in the middle and two LaO layers around it, as well as alternating layers of TiO_2 with SrO on both sides as shown in Figure 1. In this case, the supercell has two symmetric n-type interfaces and there is no potential buildup due to

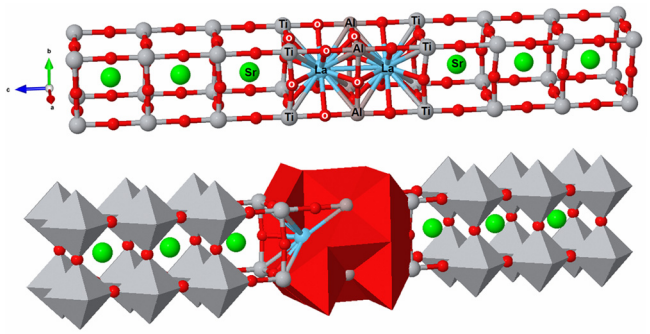

FIG. 1. Depicted the type of symmetric structure, with two identical interfaces, it is assumed that a perfect STO layer (with TiO_2-LaO planes at the interface) can be deposited on top of the LaO. A symmetric model interface was employed without the vacuum layer.

symmetry. This approach automatically guarantees the doping of 1 electron in the supercell. The doped charge accumulates at the TiO_2 layers at the interface and results in a doping of 0.5 e−/uc. The results can be compared to the experimental case of a single n-type interface with an extremely thick LAO layer. These studies could be valuable for the atomic and electronic structure of a fully reconstructed interface, but it cannot describe the potential buildup and the charge transfer, which is necessary in the experiment.[37] The feature of the symmetry-supercell way is that no vacuum is needful in the simulation of the supercell, making its calculation easier. However, because of the imposed symmetry and nonstoichiometry of the LAO film, this geometry does not lead in a polar field, meaning that a polar catastrophe can be obviated. The nonstoichiometry of the LAO also creates fixed carrier doping; in the ionic limit, a LaO layer has a charge of +1, and there is an additional one electron existing in the conduction band of LAO, which is evenly divided by the two interfaces. Therefore, each n-type interface is doped by 1/2 electron per two-dimensional unit cell, substantial to totally compensate the polar field of LAO; so the symmetric supercell way is comparable to researching the characteristics of the interfaces when the LAO film is very thick. In Figures 2(a)–2(c), we plot the electronic band structures of the two symmetric n-type 6.5STO/1.5LAO interfaces using LDA, PBE-GGA, and EVGGA approaches. Since EVGGA produces better band splitting, we have presented the total density of states (TDOS) obtained by EVGGA next to the electronic band structure of the two symmetric n-type 6.5STO/1.5LAO interfaces as shown in Figure 3. We have set the zero-point of energy at Fermi level (E_F). We discovered that some bands cross E_F, resulting in the metallic nature of the two symmetric n-type 6.5STO/1.5LAO interfaces with a density of states at E_F, $N(E_F)$, of about 3.56 (state/eV/unit cell). The calculated density of states at E_F enables us to calculate the bare electronic specific heat coefficient (γ), which is about 0.62 mJ/(mol cell K^2). To identify the origin of the bands which cross E_F, we plot the electronic band structure and the partial density of states in the closeness of E_F as shown in Figures 3(b) and 3(c). It is clear that these bands are mainly originated from Ti1,2,3,4-3dxy orbitals. Thus, these bands are responsible for the metallic behavior and the forming of the Fermi surface of the two symmetric

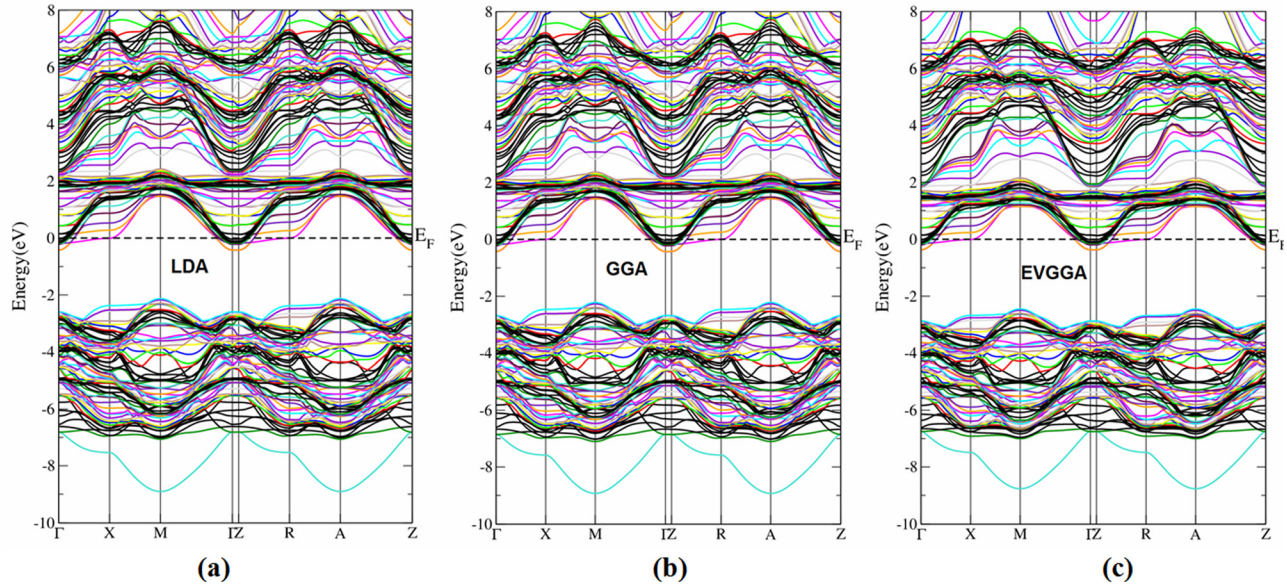

FIG. 2. Calculated electronic band structure of 6.5STO/1.5LAO using (a) LDA, (b) PBE-GGA, and (c) EVGGA.

n-type 6.5STO/1.5LAO interfaces. This planner leads to a transition from states that insulate to metallic ones. In the present LDA, PBE-GGA, and EVGGA computations, the metallic state occurs at N(LaO) = 2 and experiments clarify that bilayers with N(LaO) = 3 for the n-type interface are still nonconducting, while LAO films with $N(LaO) \geq 4$ have been explored to be metallic. Consequently, one electron per interface is necessary in order to preserve the neutrality of the system. The Ti1,2,3,4-3dxy orbitals in the plane neighboring to the interface have a limited density of states at Fermi energy level and remain metallic, regardless of the amount of unit cells in the LAO film.

At the n-type interface, the STO conduction band is lessened because of the chemical bonding in the Ti and La and oxygen octahedra deformation, while the valence band is raised due to the induced polarization.[30] Electrons at the n-type interface are confined to the interface.[38] To model isolated interfaces (IFs), it has been an exercise to utilize the symmetrical supercells, i.e., two are opposing n-type IFs in the supercell. Then, by the influence of symmetry, there is no dipole in the cell and the periodically supercell processing is applicable. Again, the usage of symmetric supercells is simple; each half of the cell may have a dipole as specified by the geometry and the self-consistent response to electric fields, whereas the opposing dipoles leave a slab that can be treated in the periodically supercell. The question still exists as to what range these can be recognized in an experiment. STO/LAO double heterostructures, with mirror-symmetric TiO_2/LaO interfaces, will result in a DEG density equivalent to 1/2 an electron per unit cell at each interface. This can be illustrated depending on the symmetry of the structure, which forces a nearly flat electrostatic potential over the LAO layer. Gauss' law then states that the net charge density at each interface (integrated over the width of the 2DEG) has to be zero, i.e., no electrons infiltrate away from the interface. In STO/LAO, growing such symmetric interfaces has been confirmed to be very hard.[11] For the double n-type symmetric supercells, which owns no polar fields and in which there are no holes existing to innovate electrostatic attraction, DFT simulation still detects limited electron gas at the interface. This has already been presented in Refs. 32 and 39. For symmetric supercells with no polar fields, it would be expected that the electrons would occupy the lower-energy conduction band edge of the two substances and would distribute over the substrate.

In this interface, E_F is in the conduction band, as expected, because of the formal charge in the LaO slab. The state near E_F is fundamentally consisting of Ti-3 d states at the interface. The n-type metallicity in this superlattice is a consequence of the charge transfer from the $(LaO)^+$ layer to the $(TiO_2)^0$ layer. This is recognized by the Ti-mixed valency at the interface. The symmetrical nature of the charge density in the STO layer is a result of our first-principles computation needing to preserve periodicity over the (001) direction, and thus corresponds a superlattice including two interfaces. The type of symmetric structure is shown in Figure 1, with two similar interfaces, is never accomplished in experiment. In most practical applications, the LAO layer is of limited thickness. In Figure 1, it is supposed that an ideal STO layer (with TiO_2-LaO planes at the interface) can be put on top of the LaO. Empirically, it is not easy to cultivate STO/LAO/STO structures with an interface between LaO and TiO_2 planes; therefore, a symmetrical model interface was utilized, without the vacuum layer. As there are two interfaces within the model, each interface receives an equal half of an electron. In this type of model structure, the amount of electron transfer is not dependent on the LAO thickness, in contrast to the outcomes that relied on the stoichiometric LAO and STO slabs.

We have calculated the effective mass of electrons (m_e^*) from the calculated band structure of the two symmetric n-type 6.5STO/1.5LAO interface (Fig. 3(c)). Usually, we estimated the value of m_e^* from the conduction band minimum curvature. The diagonal elements of the effective mass tensor, m_e, for the electrons in the conduction band are calculated in the following expression:

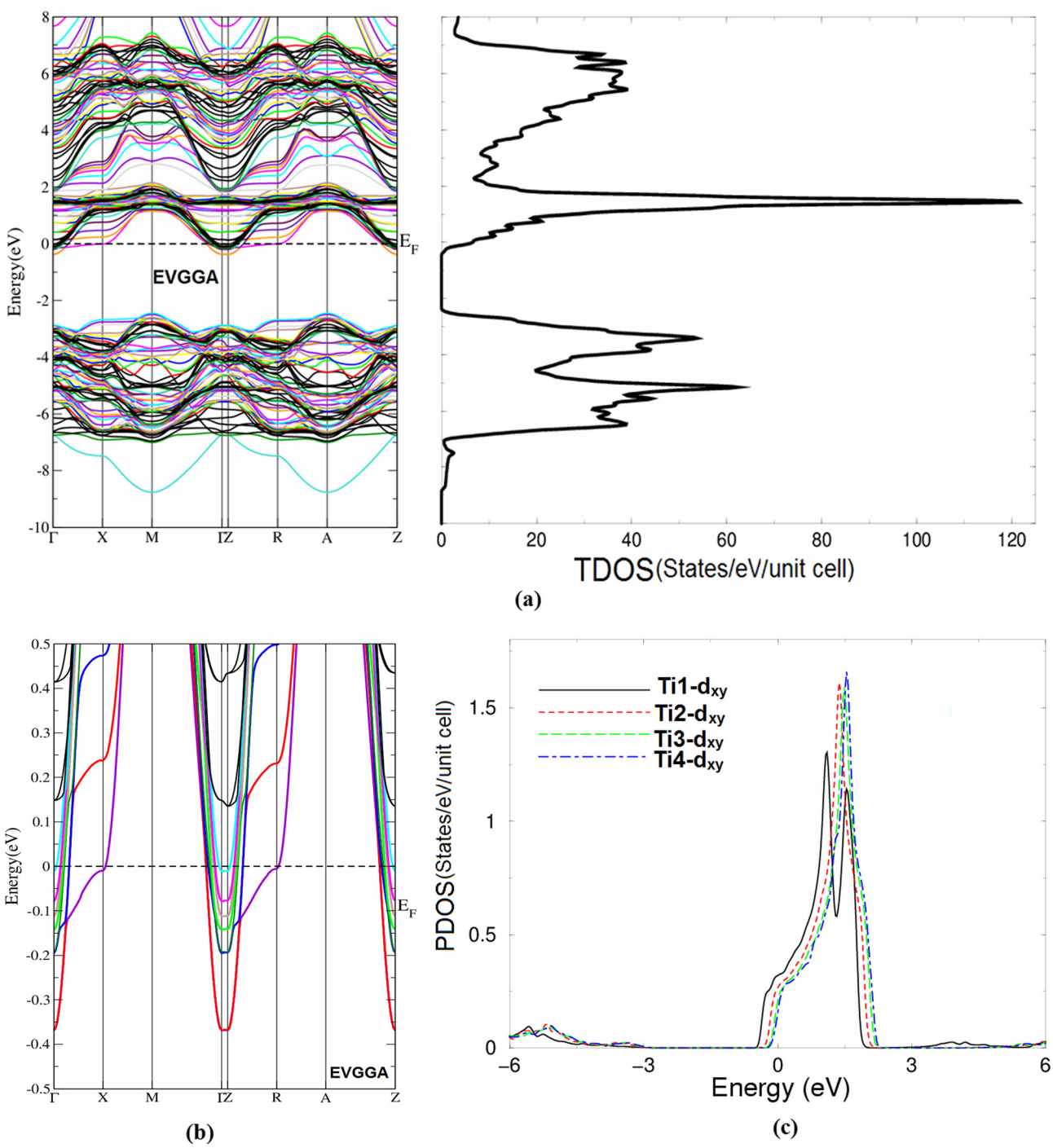

FIG. 3. (a) Calculated electronic band structure of 6.5STO/1.5LAO along with the total density of states using EVGGA. (b)–(c) Calculated electronic band structure of 6.5STO/1.5LAO superlattices along with the Ti1,2,3,4-3dxy partial density of states in the vicinity of Fermi level.

$$\frac{1}{m_e^*} = \frac{1\partial^2 E(k)}{\hbar^2 \partial k^2}. \quad (1)$$

The effective mass of electron is assessed by fitting the electronic band structure to a parabolic function, Eq. (1). The calculated electron effective mass ratio (m_e^*/m_e) around Γ point of BZ is about 0.0249, 0.0257, 0.0411, and 0.0315 for Ti1-d_{xy}, Ti2-d_{xy}, Ti3-d_{xy}, and Ti4-d_{xy}, respectively, which implies that the bands in the vicinity of Fermi level (E_F) possess low effective masses (m^*) resulting in high mobility carriers and hence high electrical conductivity in good agreement with pervious work.[28,40]

Figure 3(c) lays out the amendments of the projected density of the state of Ti in the layer neighboring to the interface (Ti1) and in a further distance (4th) layer (Ti4). In the interface layer, the relaxation results in a small shift of the conduction 3dxy band to the low-energy region and, more substantially, to a decrease DOS adjacent to the Fermi energy level which proposes a decrease in the density of the charge carrier. Compared to the interface TiO_2, the relaxed

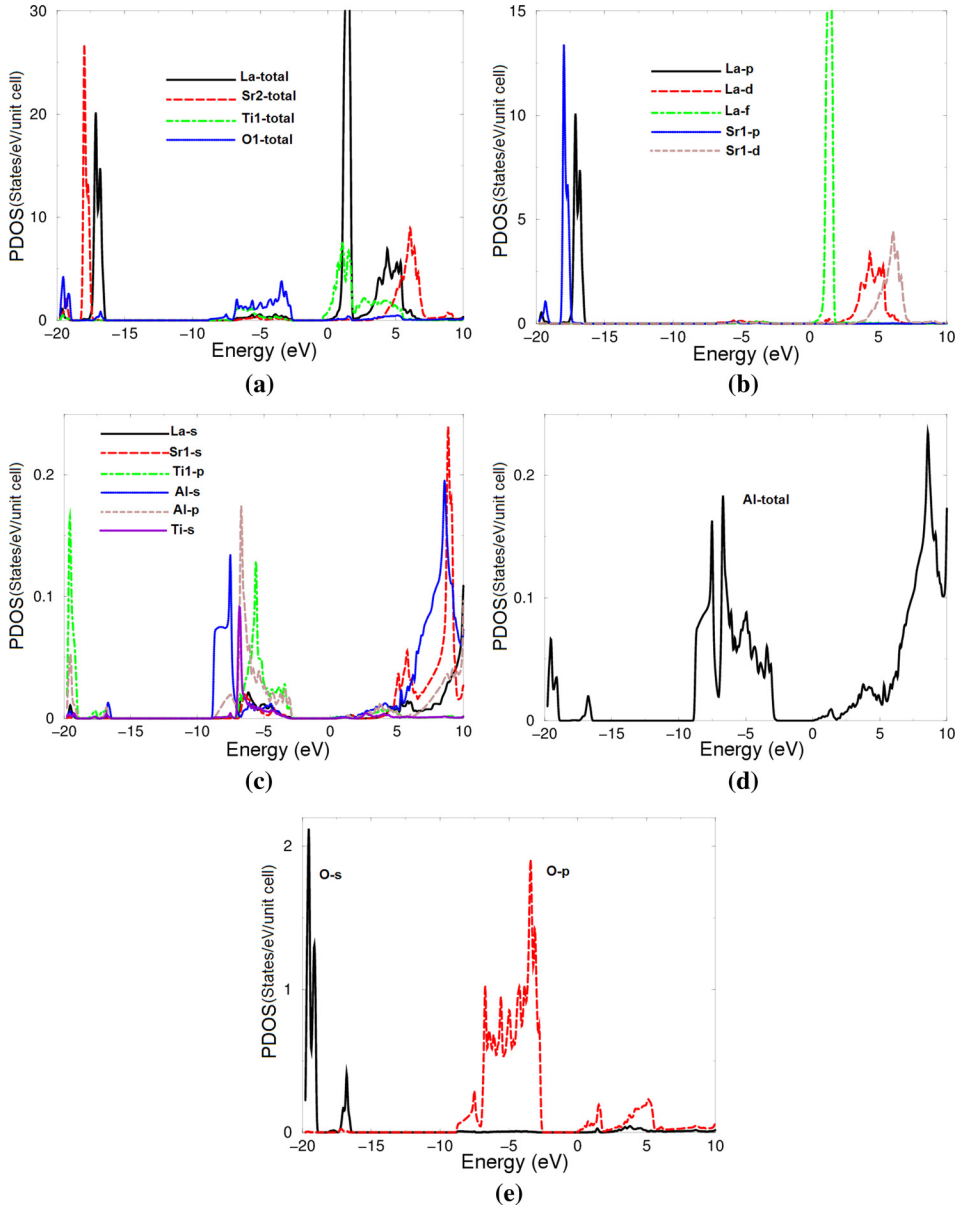

FIG. 4. Calculated partial density of states for 6.5STO/1.5LAO using EVGGA.

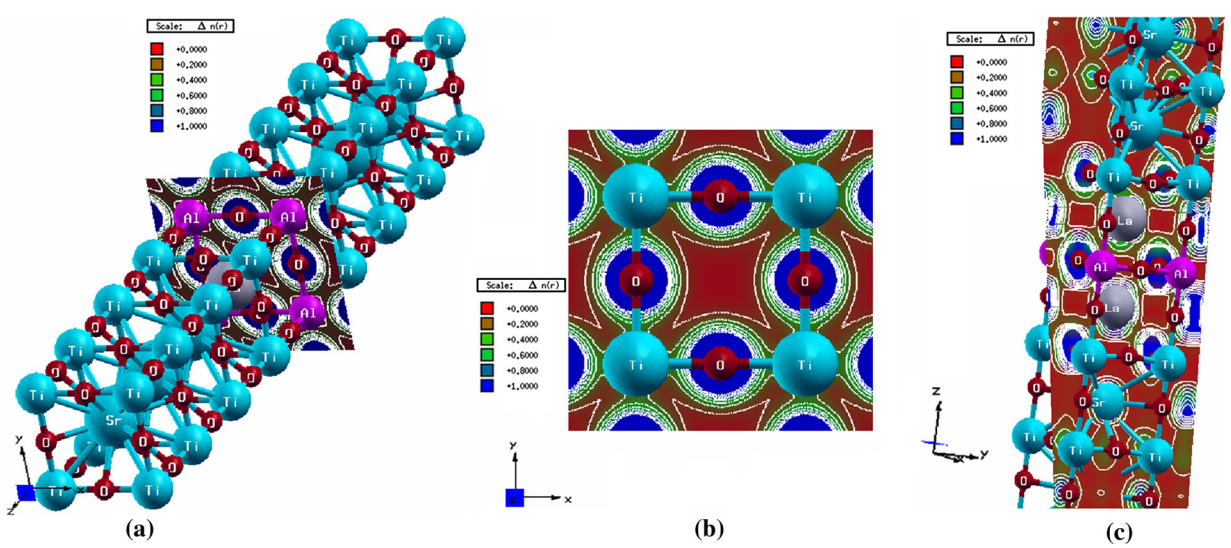

FIG. 5. Calculate total valence charge density distribution for 6.5STO/1.5LAO.

3dxy band of Ti4 is moved further below the Fermi energy level and the DOS at the Fermi energy level is strengthened. The shifting conduction bands also create changes in their particular charge occupancies. The fact that the Ti 3 d state is partially occupied reveals that there is mixed valency of +3 and +4 in Ti. The accumulation of metallic states moves through the manifestation of the electron carriers in the Ti $3d_{xy}$ bands. This is escorted by filling up the gap which, for N(LaO) = 2, exists between the oxygen 2 p and the La 5 d and Ti 3 d bands. The 2 p states of the oxygen in the AlO_2 planes approach the Fermi energy from below, while the interface Ti 3dxy states cross the Fermi energy level from above.

The largest addition to the occupied states near E_F comes from the interfacial Ti ion, with the rest of the Ti

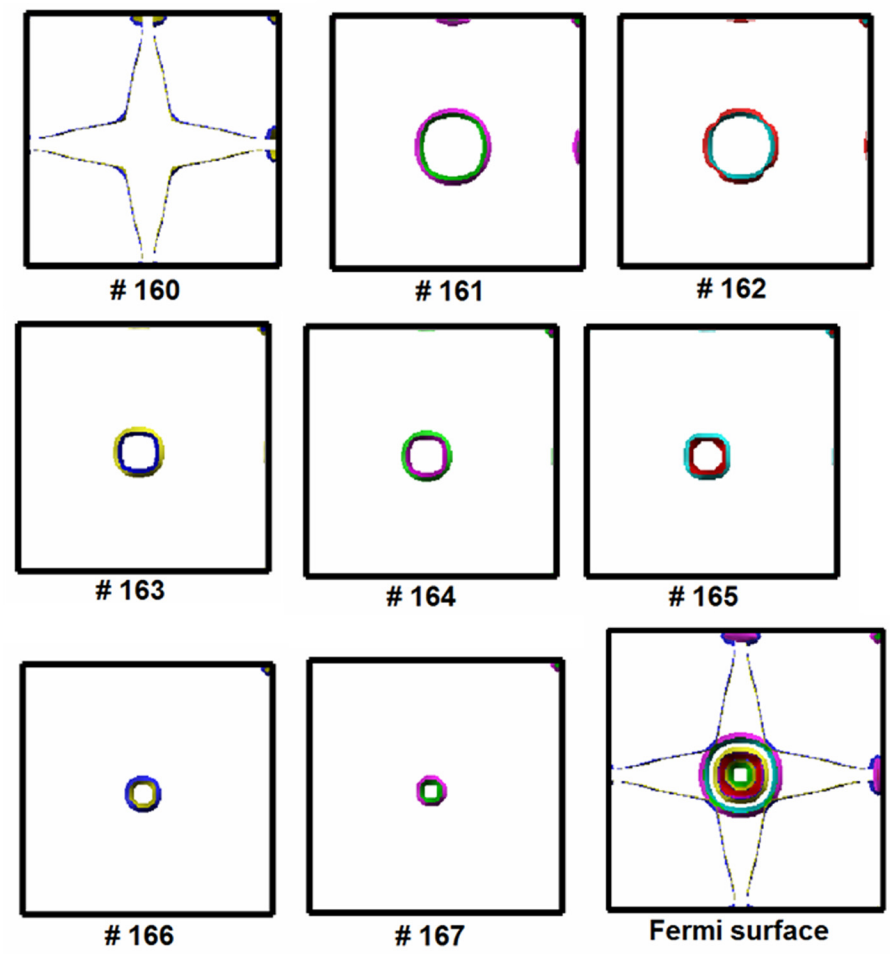

FIG. 6. (a) and (b) Calculated Fermi surface for 6.5STO/1.5LAO interface using EVGGA.

atoms participating less as the distance to the interface rises. This is correct for LDA, PBE-GGA, and EVGGA approximations. There is no contribution from the interfacial La ions to the occupied states, as that peak is displaced towards the right in comparison to the La atom at the free surface of the sheet. There is one electron per two symmetric n-type interfaces that participates in the 2DEG, and this electron is distributed out through five Ti layers on either side of the interface. In Figures 3(a) and 3(b), E_F crosses four d_{xy} bands of the first four Ti atoms from the interface. A general understanding of the conducting mechanism at oxide interfaces is a crucial prerequisite for the development of real electronic devices and applications. The origin of the high concentration of electronic charge carriers at the interface between LAO and STO is still the topic of controversial debate.

To further understand the physical properties of the two symmetric n-type 6.5STO/1.5LAO interfaces, the angular momentum solved projected density of states is also investigated as is illustrated in Figure 4. It has been noticed that there exists a sturdy hybridization between La-s with Ti-s, Sr-s with Al-s, Ti-p with Al-p states, and Al-p with Ti-s. The hybridization may result in the formation of covalent bonding and the strengths of the covalency will depend on the degree of hybridization. To support this statement, we have investigated the bond's nature and the interactions between the atoms as shown in Figures 5(a)–5(c). Following these figures, we obtained a clear map of the valence band electronic charge density distribution of the two symmetric n-type 6.5STO/1.5LAO interfaces in three crystallographic planes, namely, (0 0 1), (1 0 0), and (1 1 0). The (0 0 1) crystallographic plane (Figure 5(a)) shows the O and Al atoms exhibit weak covalent bonding, and the O atoms are surrounded by a spherical charge. It has been observed that the (1 0 0) plane (Figure 5(b)) exhibits only O and Ti atoms; the O atoms are surrounded by a spherical charge and the outer shell forms weak covalent bonds with the nearest Ti atoms. Therefore, the bond between O-Ti is mostly ionic and partially covalent due to the Pauling electronegativity differences between Ti (1.54) and O (3.44). Whereas the (1 1 0) (Figure 5(c)) plane exhibits all the atoms, and it has been noticed that La atoms form ionic bonding while Sr atoms form weak covalent bonds with O atoms. Due to electronegativity differences between La (1.1), Al (1.61), Ti (1.54), Sr (0.95), and O (3.44), one can notice that the charge is attracted across O atoms which is obviously displayed by the blue (1.0000) color corresponding to the maximum charge accumulation site in accordance with the charge density scale.

It was earlier mentioned that the calculated electronic band structure shows that there are some bands crossing the Fermi level to form a Fermi surface in accordance with our observation of partial density at the Fermi level. These bands consist mainly of Ti1,2,3,4-3dxy states with some other states. The Fermi level is identified by the Kohn–Sham eigenvalues of the highest occupied state. The Fermi surface is displayed in Figures 6(a) and 6(b). The observed Fermi surface composes of empty regions that represent the gaps and shaded regions corresponding to the electrons.

IV. CONCLUSIONS

We have explored the electronic structure of the two symmetric n-type 6.5STO/1.5LAO interfaces using the all-electron full potential linearized augmented plane wave plus the local orbitals (FP-LAPW+lo) approach based on the density-functional theory. The metallic state is acquired for the relaxed structure of a superlattice with the $(LaO)^{+}/(TiO_2)^{0}$ interface using LDA, PBE-GGA, and EVGGA approximations. Ionic relaxation plays a significant role in forming the localization of the extra electron on the interface Ti ions and infiltration into the bulk layer. Analysis of the total and projected DOS indicates that states near E_F are due to the Ti-3 d states at the two symmetric n-type interfaces. We focused on the interaction between Ti and La at the interface. The strong interfacial hopping triggers a rise in the energy of the La d_{xy} state, and a lowering in the energy of the Ti d_{xy} state. Compared to the other Ti orbitals in the substrate, the Ti d orbitals at the two symmetric n-type interfaces are appropriate because they have more energy and are thus able to more effectively bind electrons to the interface. In the language of chemistry, a couple of bonding and antibonding states between the two cations are formed at the interface. The calculated valence band electronic charge density distribution of the two symmetric n-type 6.5STO/1.5LAO interfaces helps to investigate the bond's nature, charge transfer, and the interactions between the atoms. The calculated valence band electronic charge density reveal that the charge is attracted towards O atoms which are surrounded by uniform blue spheres which indicate the maximum charge accumulation.

ACKNOWLEDGMENTS

A. H. Reshak would like to acknowledge the CENTEM Project, Reg. No. CZ.1.05/2.1.00/03.0088, cofunded by the ERDF as part of the Ministry of Education, Youth and Sports OP RDI programme and, in the follow-up sustainability stage, supported through CENTEM PLUS (LO1402) by financial means from the Ministry of Education, Youth and Sports under the "National Sustainability Programme I." Computational resources were provided by MetaCentrum (LM2010005) and CERIT-SC (CZ.1.05/3.2.00/08.0144) infrastructures. Y.A. would like to thank University Malaysia Perlis for Grant No. 9007-00185 and TWAS-Italy for the full support of his visit to JUST-Jordan under a TWAS-UNESCO Associateship. M. S. Abu-Jafar would like to acknowledge the fruitful discussions with M. Grilli, S. Caprara, and Z. Zhong.

[1]A. Ohtomo and H. Y. Hwang, "A high-mobility electron gas at the $LaAlO_3/SrTiO_3$ Heterointerface," Nature (London) **427**, 423 (2004).
[2]D. A. Dikin, M. Mehta, C. W. Bark, C. M. Folkman, C. B. Eom, and V. Chandrasekhar, "Coexistence of superconductivity and ferromagnetism in two dimensions," Phys. Rev. Lett. **107**, 056802 (2011).
[3]C. Cen, S. Thiel, G. Hammerl, C. W. Schneider, K. E. Andersen, C. S. Hellberg, J. Mannhart, and J. Levy, "Nanoscale control of an interfacial metal–insulator transition at room temperature," Nat. Mater. **7**, 298 (2008).
[4]M. Huijben, A. Brinkman, G. Koster, G. Rijnders, H. Hilgenkamp, and H. A. Blank, "Structure–property relation of $SrTiO_3/LaAlO_3$ interfaces," Adv. Mater. **21**, 1665 (2009).

[5]N. Nakagawa, H. Y. Hwang, and D. A. Muller, "Why some interfaces cannot be sharp," Nat. Mater. **5**, 204 (2006).

[6]H. Wadati, J. Geck, D. G. Hawthorn, T. Higuchi, M. Hosoda, C. Bell, Y. Hikita, H. Y. Hwang, C. Schussler-Langeheine, E. Schierle, E. Weschke, and G. A. Sawatzky, "Electronic structure of the $SrTiO_3/LaAlO_3$ interface revealed by resonant soft x-ray scattering," IOP Conf. Ser.: Mater. Sci. Eng. **24**, 012012 (2011).

[7]R. Hesper, L. H. Tjeng, A. Heeres, and G. A. Sawatzky, "Photoemission evidence of electronic stabilization of polar surfaces in K_3C_{60}," Phys. Rev. B **62**, 16046 (2000).

[8]P. R. Willmott, S. A. Pauli, R. Herger, C. M. Schlepütz, D. Martoccia, B. D. Patterson, B. Delley, R. Clarke, D. Kumah, C. Cionca, and Y. Yacoby, "Structural basis for the conducting interface between $LaAlO_3$ and $SrTiO_3$," Phys. Rev. Lett. **99**, 155502 (2007).

[9]Z. Erlich, Y. Frenkel, J. Drori, Y. Shperber, C. Bell, H. K. Sato, M. Hosoda, Y. Xie, Y. Hikita, H. Y. Hwang, and B. J. Kalisky, "Optical study of tetragonal domains in $LaAlO_3$/SrTiO3," Supercond. Nov. Magn. **28**, 1017 (2015).

[10]M. Salluzzo, J. C. Cezar, N. B. Brookes, V. De Bisogni, G. M. Luca, C. Richter, S. Thiel, J. Mannhart, M. Huijben, A. Brinkman, G. Rijnders, and G. Ghiringhelli, "Orbital reconstruction and the two-dimensional electron gas at the $LaAlO_3/SrTiO_3$ interface," Phys. Rev. Lett. **102**, 166804 (2009).

[11]M. Huijben, G. Rijnders, D. H. A. Blank, S. Bals, S. V. Aert, J. Verbeeck, G. V. Tendeloo, A. Brinkman, and H. Hilgenkamp, "Electronically coupled complementary interfaces between perovskite band insulators," Nat. Mater. **5**, 556 (2006).

[12]S. Thiel, G. Hammerl, A. Schmehl, C. W. Schneider, and J. Mannhart, "Tunable quasi-two-dimensional electron gases in oxide heterostructures," Science **313**, 1942 (2006).

[13]G. Herranz, M. Basletic, M. Bibes, C. Carretero, E. Tafra, E. Jacquet, K. Bouzehouane, C. Deranlot, A. Hamzic, J.-M. Broto, A. Barthelemy, and A. Fert, "high mobility in $LaAlO_3/SrTiO_3$ heterostructures: Origin, dimensionality, and perspectives," Phys. Rev. Lett. **98**, 216803 (2007).

[14]W. Siemons, G. Koster, H. Yamamoto, W. A. Harrison, G. Lucovsky, T. H. Geballe, D. H. A. Blank, and M. R. Beasley, "Origin of charge density at $LaAlO_3$ on $SrTiO_3$ heterointerfaces: Possibility of intrinsic doping," Phys. Rev. Lett. **98**, 196802 (2007).

[15]A. Kalabukhov, R. Gunnarsson, J. Borjesson, E. Olsson, T. Claeson, and D. Winkler, "Effect of oxygen vacancies in the $SrTiO_3$ substrate on the electrical properties of the $LaAlO_3/SrTiO_3$ interface," Phys. Rev. B **75**, 121404 (2007).

[16]M. Balestic, J.-L. Maurice, C. Carretero, G. Herranz, O. Copie, M. Bibes, E. Jacquet, K. Bouzehouane, S. Fusil, and A. Barthelemy, "Mapping the spatial distribution of charge carriers in $LaAlO_3/SrTiO_3$ heterostructures," Nat. Mater. **7**, 621 (2008).

[17]K. Yoshimatsu, R. Yasuhara, H. Kumigashira, and M. Oshima, "Origin of metallic states at the heterointerface between the band insulators $LaAlO_3$ and $SrTiO_3$," Phys. Rev. Lett. **101**, 026802 (2008).

[18]M. Sing, G. Berner, K. Goss, A. Muller, A. Ruff, A. Wetscherek, S. Thiel, J. Mannhart, S. A. Pauli, C. W. Schneider, P. R. Willmott, M. Gorgoi, F. Schafers, and R. Claessen, "Profiling the interface electron gas of $LaAlO_3/SrTiO_3$ heterostructures by hard X-ray photoelectron spectroscopy," Phys. Rev. Lett. **102**, 176805 (2009).

[19]R. Pentcheva and W. E. Pickett, "Charge localization or itineracy at $LaAlO_3/SrTiO_3$ interfaces: Hole polarons, oxygen vacancies, and mobile electrons," Phys. Rev. B **74**, 035112 (2006).

[20]M. S. Park, S. H. Rhim, and A. J. Freeman, "Charge compensation and mixed valency in $LaAlO_3/SrTiO_3$ heterointerfaces studied by the FP-LAPW method," Phys. Rev. B **74**, 205416 (2006).

[21]S. Ishibashi and K. Terakura, "Analysis of screening mechanisms for polar discontinuity for $LaAlO_3/SrTiO_3$ thin films based on *ab initio* calculations," J. Phys. Soc. Jpn. **77**, 104706 (2008).

[22]S. A. Chambers, "Understanding the mechanism of conductivity at the $LaAlO_3/SrTiO_3$ (001) interface," Surf. Sci. **605**, 1133–1140 (2011).

[23]N. Reyren, S. Thiel, A. D. Caviglia, L. F. Kourkoutis, G. Hammer, C. Richter, C. W. Schneider, T. Kopp, A.-S. Ruetschi, D. Jaccard, M. Gabay, D. A. Muller, J.-M. Triscone, and J. Mannhart, "Superconducting interfaces between insulating oxides," Science **317**, 1196 (2007).

[24]A. Brinkman, M. Huijben, M. van Zalk, J. Huijben, U. Zeitler, J. C. Maan, W. G. van der Wiel, G. Rijnders, D. H. A. Blank, and H. Hilgenkamp, "Magnetic effects at the interface between non-magnetic oxides," Nat. Mater. **6**, 493 (2007).

[25]S. Lerer, M. Ben Shalom, G. Deutscher, and Y. Dagan, "Low-temperature dependence of the thermomagnetic transport properties of the $SrTiO_3/LaAlO_3$ interface," Phys. Rev. B **84**, 075423 (2011).

[26]I. Pallecchi, M. Codda, E. Galleani d'Agliano, D. Marre, A. D. Caviglia, N. Reyren, S. Gariglio, and J.-M. Triscone, "Seebeck effect in the conducting $LaAlO_3/SrTiO_3$ interface," Phys. Rev. B **81**, 085414 (2010).

[27]A. Filippetti, P. Delugas, M. J. Verstraete, I. Pallecchi, A. Gadaleta, D. Marre, D. F. Li, S. Gariglio, and V. Fiorentini, "Thermopower in oxide heterostructures: The importance of being multiple-band conductors," Phys. Rev. B **86**, 195301 (2012).

[28]P. Delugas, A. Filippetti, V. Fiorentini, D. I. Bilc, D. Fontaine, and P. Ghosez, "Spontaneous two-dimensional carrier confinement at the n-type $SrTiO_3/LaAlO_3$ interface," Phys. Rev. Lett. **106**, 166807 (2011).

[29]Z. Zhong, A. Toth, and K. Held, "Theory of spin-orbit coupling at $LaAlO_3/SrTiO_3$ interfaces and $SrTiO_3$ surfaces," Phys. Rev. B **87**, 161102(R) (2013).

[30]Z. Zhong, P. Wissgott, K. Held, and G. Sangiovanni, "Microscopic understanding of the orbital splitting and its tuning at oxide interfaces," EPL **99**, 37011 (2012).

[31]R. Arras, V. G. Ruiz, W. E. Pickett, and R. Pentcheva, "Tuning the two-dimensional electron gas at the $LaAlO_3/SrTiO_3$(001) interface by metallic contacts," Phys. Rev. B **85**, 125404 (2012).

[32]Z. S. Popovic, S. Satpathy, and R. M. Martin, "Origin of the two-dimensional electron gas carrier density at the $LaAlO_3$ on $SrTiO_3$ interface," Phys. Rev. Lett. **101**, 256801 (2008).

[33]J. P. Perdew and Y. Wang, "Accurate and simple analytic representation of the electron-gas correlation energy," Phys. Rev. B **45**, 13244 (1992).

[34]J. P. Perdew, S. Burke, and M. Ernzerhof, "Generalized gradient approximation made simple," Phys. Rev. Lett. **77**, 3865 (1996).

[35]E. Engel and S. H. Vosko, "Exact exchange-only potentials and the virial relation as microscopic criteria for generalized gradient approximations," Phys. Rev. B **47**, 13164 (1993).

[36]P. Blaha, K. Schwarz, G. K. H. Madsen, D. Kvanicka, and J. Luitz, *WIEN2K, An Augmented plane wave + Local Orbital Program for Calculating Crystal Properties* (Technische Universitat, Wien, Austria, 2001); ISBN: 3-9501031-1-1-2.

[37]J. Lee and A. Demkov, "Charge origin and localization at the *n*-type $SrTiO_3/LaAlO_3$ Interface," Phys. Rev. B **78**, 193104 (2008).

[38]J. M. Albina, M. Mrovec, B. Meyer, and C. Elsaesser, "Structure, stability, and electronic properties of $SrTiO_3/LaAlO_3$ and $SrTiO_3/SrRuO_3$ interfaces," Phys. Rev. B **76**, 165103 (2007).

[39]K. Janicka, J. P. Velev, and E. Y. Tsymbal, "Quantum nature of two-dimensional electron gas confinement at $LaAlO_3/SrTiO_3$ interfaces," Phys. Rev. Lett. **102**, 106803 (2009).

[40]W.-J. Son, E. Cho, B. Lee, J. Lee, and S. Han, "Density and spatial distribution of charge carriers in the intrinsic ***n***-type LaAlO3-SrTiO3 interface," Phys. Rev B **79**, 245411 (2009).